Nanomedicine

DOI: 10.1002/ange.201106758

Anchored Proteinase-Targetable Optomagnetic Nanoprobes for Molecular Imaging of Invasive Cancer Cells**

Joseph Park, Jaemoon Yang, Eun-Kyung Lim, Eunjung Kim, Jihye Choi, Joo Kyung Ryu, Nam Hee Kim, Jin-Suck Suh, Jong In Yook, Yong-Min Huh, and Seungjoo Haam**

Matrix metalloproteinases (MMPs) are attractive targets for molecular imaging because degrading and modifying the extracellular matrix by enzymatic activity is required for the invasive process of cancer cells.[1] Among the large family of MMPs, increasing evidence suggests that a subclass of the membrane-anchored proteinases, the membrane-type (MT) MMPs, plays dominant roles in controlling invasive cancer cell behavior.[2] In particular, MT1-MMP not only plays a direct and essential role in allowing tumor cells to invade into connective tissue,[2,3] but also provides a direct cellular target for molecular imaging to detect invasive cancer cells, in comparison with secreted, soluble MMPs.[1a,2,3]

Herein, we describe the development of a bimodal imaging probe enabling precise recognition of the expression of MT1-MMP anchored on invasive cancer cells and its protease activity simultaneously. MT1-MMP may be a targetable biomarker for a specific delivery and possesses proteolytic activity for certain substrates.[4] Activatable fluorogenic peptide (ActFP) was formulated as a targeting moiety and proteolytic ligand for MT1-MMP and conjugated with magnetic nanocrystals (MNCs), synthesized as magnetic resonance (MR) imaging contrast agents (Figure 1).[5] The magnetic and fluorogenic properties, based on the fluorescence resonance energy transfer (FRET) effect, of MNC-ActFP and their targeting potential were investigated to assess its capability as a multimode imaging probe.[6]

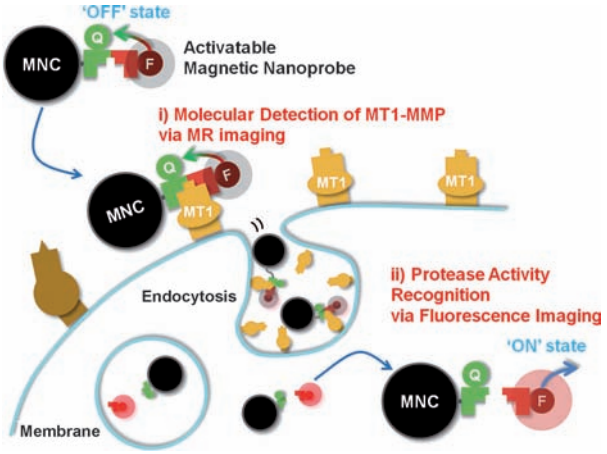

Figure 1. The dual imaging process of activatable magnetic nanoprobes (magnetic nanocrystals conjugated with activatable fluorogenic peptides, MNC-ActFP) for i) molecular detection of MT1-MMP anchored on invasive cancer cells by MR imaging, and ii) sensitive recognition of the proteolytic activity of MT1-MMP by fluorescence imaging. Q = quencher, F = fluorescence dye.

For targeted imaging of MT1-MMP anchored on invasive cancer cells and the measurement of the prolyteolytic activity, ActFP (Cy5.5-GPLPLRSWGLK(BHQ-3)) was designed and synthesized as both a MT1-MMP-specific substrate and a fluorescence imaging probe, based on the FRET effect (Supporting Information, Figure S1). First, a shorter fluorogenic peptide was prepared by labeling at both ends to form Cy5.5-GPLPLRSW(BHQ-3) amide. However, because of the bulky structures of Cy5.5 and BHQ-3, peptide cleavage was not observed. Considering this steric hinderance, we modified the fluorogenic peptide by inserting three amino acid sequence spacers (GLK) for effective cleavaging to MT1-MMP (Supporting Information, Figure S2).[4a,7] MNCs, as MR imaging contrast agents, were synthesized by a thermal decomposition method and were coated with aminated polysorbate for the solubilization into the aqueous phase and the conjugation of ActFP.[8] After the conjugation of ActFP to the aminated MNCs using the carbodiimide EDC, the colloidal size of MNC-ActFP was 42.3 ± 1.2 nm, by laser scattering, which was slightly larger than bare water-soluble MNCs (37.3 ± 2.2 nm). Furthermore, MNC-ActFP exhibited a negative surface charge at -8.2 ± 3.7 mV, which was converted from the positive surface charge of the aminated MNC (24 ± 5.2 mV) owing to the conjugation of anionic

[*] J. Park,[+] E.-K. Lim, E. Kim, J. Choi, Prof. S. Haam
Department of Chemical and Biomolecular Engineering
Yonsei University, Seoul 120-749 (Republic of Korea)
E-mail: haam@yonsei.ac.kr
Prof. J. Yang,[+] Prof. J.-S. Suh, Prof. Y.-M. Huh
Department of Radiology, Yonsei University
Seoul 120-752 (Republic of Korea)
E-mail: ymhuh@yuhs.ac
J. K. Ryu, N. H. Kim, Prof. J. I. Yook
Department of Oral pathology, Oral Cancer Research Institute
Yonsei University, Seoul 120-752 (Republic of Korea)
Prof. J. Yang,[+] Prof. J.-S. Suh, Prof. Y.-M. Huh, Prof. S. Haam
YUHS-KRIBB Medical Convergence Research Institute
Seoul 120-752 (Republic of Korea)
Prof. J.-S. Suh, Prof. Y.-M. Huh
Severance Biomedical Science Institute (SBSI)
Seoul 120-749 (Republic of Korea)
[+] These authors contributed equally to this work.

[**] This work was supported by the Korea Science and Engineering Foundation grant funded by the Korean government (M10755020001-07N5502-00110), the KRIBB Research Initiative Program (7-2009-0326), National Research Foundation of Korea Grant funded by the Korean Government (MEST) (2010-0019923) and a grant of the Korea Healthcare technology R&D Project, Ministry for Health & Welfare Affairs, Republic of Korea (A085136)
Supporting information for this article is available on the WWW under http://dx.doi.org/10.1002/anie.201106758.

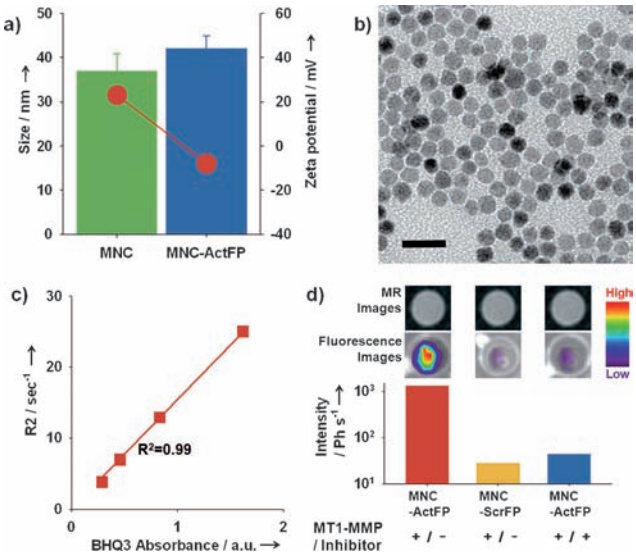

Figure 2. a) Size (bar) and zeta potential (line–scatter) of MNC and MNC-ActFP. b) TEM image of MNC-ActFP. Scale bar: 50 nm. c) Correlation graph for $R2$ ($1/T2$) versus the BHQ3 absorbance at 690 nm of MNC-ActFP. d) MR images, fluorescence images, and fluorescence intensity graph for MNC-ActFP, MNC-ScrFP, and MNC-ActFP plus inhibitor (GM6001) treated with MT1-MMP after 60 min incubation at 37 °C.

ActFP (Figure 2a). The morphology of MNC-ActFP was confirmed by a transmission electron microscopy (TEM) image (Figure 2b). The relaxivity coefficient ($r2$) from the spin–spin relaxation time ($T2$) weighted MR images for MNC-ActFP was 404.75 $mM^{-1}s^{-1}$ and MR signal sensitivity was linearly proportional to the concentration of BHQ3 from MNC-ActFP (Figure 2c).

To investigate the specificity and proteolytic activity of MT1-MMP, MNC-ActFP as a substrate was treated with MT1-MMP, MMP3, and MMP7 at 37 °C for 1 h. As seen in Figure 2d, MT1-MMP exhibited over 500-fold higher proteolytic activity for MNC-ActFP than other proteases (MMP3 and MMP7; Supporting Information, Figure S6). To assess the selectivity for MNC-ActFP, we also further prepared a scrambled fluorogenic peptide (ScrFP, Cy5.5-GPLPERSWGLK(BHQ-3)). MNC-ScrFP was formulated in a similar manner to MNC-ActFP. Figure 2d shows that MNC-ScrFP did not exhibit strong fluorescence intensity after treatment with MT1-MMP owing to the unrecognized peptide sequence. In the presence of the broad-spectrum MMP inhibitor GM6001, the fluorescence intensity for MNC-ActFP was not increased, which is consistent with the fluorescence activity depending on the proteolytic activity of MT1-MMP. In MR images (Figure 2d), however, there was no signal difference for MNC-ActFP after treatment with each MMP. These results suggest that MNC-ActFP was suitable for the intended use with the combination of MNCs for MR imaging and the activatable fluorogenic probe. In particular, MNC-ActFP demonstrated specificity and sensitive proteolytic activity with MT1-MMP for the molecular imaging of invasive cancers.

We then determined the in vitro targeting potential and fluorogenic activity of MNC-ActFP for MT1-MMP-expressing cancer cells. First, the biocompatibility of MNC-ActFP was investigated using HT1080 cells expressing endogenous MT1-MMP. We found that MNC-ActFP was not toxic upto 50 $\mu g\,mL^{-1}$ (Supporting Information, Figure S7). MNC-ActFP was specifically attached to MT1-MMP-expressing HT1080 cells (Figure 3a); this was confirmed by $T2$-weighted MR imaging. $\Delta R2/R2_{nontreatment}$ for HT1080 cells treated with MNC-ActFP was 263.1%, whereas MNC-ScrFP did not exhibit a significant increase in MR signal intensity ($\Delta R2/R2_{nontreatment} = 18.4\%$; Figure 3b). Moreover, when the inhibitor (GM6001) was co-administered with MNC-ActFP to HT1080 cells, no increase in MR signal was observed, owing to the blocking of proteolysis of MT1-MMP by MNC-ActFP (Figure 3a,b). On the other hand, the magnetic ion (Fe + Mn) contents for HT1080 cells treated with MNC-ActFP, MNC-ScrFP, and MNC-ActFP plus inhibitor were measured by inductively coupled plasma atomic emission spectroscopy.

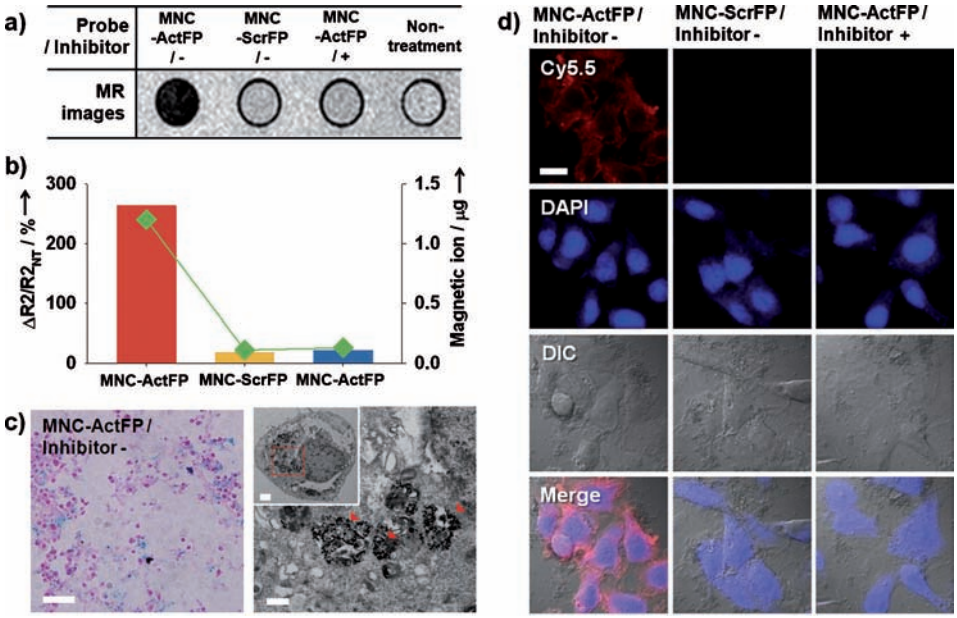

Figure 3. a) $T2$-weighted MR images for HT1080 cells treated with MNC-ActFP, MNC-ScrFP, and MNC-ActFP plus inhibitor (GM6001) and nontreated HT1080 cells. b) $\Delta R2/R2_{nontreatment}$ (bar) and magnetic ion (Fe + Mn) quantification, based on ICP-AES analysis (line scatter) for HT1080 cells treated with MNC-ActFP, MNC-ScrFP, and MNC-ActFP plus inhibitor. c) Prussian blue stained image (left; scale bar: 100 μm) and TEM images (right; scale bar: 1 μm) for HT1080 cells treated with MNC-ActFP. Low-magnification TEM image (inset; scale bar: 10 μm). Much MNC-ActFP was seen in the cytoplasm (red arrows). d) Confocal microscopic images of HT1080 cells treated with MNC-ActFP, MNC-ScrFP, and MNC-ActFP plus inhibitor (scale bar: 1 μm). MT1-MMP (red, Cy5.5) and nucleus (blue, DAPI).

MNC-ActFP exhibited over sixfold larger binding efficiency versus the other conditions (MNC-ScrFP and MNC-ActFP plus inhibitor; Figure 3b, right axis). As expected, these results were consistent with the MR imaging data. Furthermore, Prussian blue stained images of HT1080 cells treated with MNC-ActFP showed the presence of a high iron content, compared with the other conditions (MNC-ScrFP and MNC-ActFP plus inhibitor; Figure 3c, left; Supporting Information, Figure S8). In particular, the cellular TEM image clearly showed that MNC-ActFP was predominantly localized in the cytoplasm (Figure 3c, right), which is most likely due to the uptake of MNC-ActFP by MT1-MMP-mediated endocytosis.

To evaluate the near infrared (NIR) fluorogenic potential of the prepared activatable probe (MNC-ActFP) induced by MT1-MMP, confocal microscopic images of HT1080 cells treated with probes (MNC-ActFP, MNC-ScrFP, and MNC-ActFP plus inhibitor, respectively) were obtained (Figure 3d). At 1 h after the incubation of HT1080 cells treated with MNC-ActFP, cellular NIR fluorescence from Cy5.5 was detected in the cytoplasm. In contrast, neither of the other conditions (MNC-ScrFP and MNC-ActFP plus inhibitor) showed any significant increase in NIR fluorescence signal intensity, even after 60 minutes of incubation, reflecting the high specificity and sensitivity of MNC-ActFP for MT1-MMP-expressing cells. To further confirm the specific proteolytic activity of MNC-ActFP for MT1-MMP, MCF-7 cells (a cell type that expresses minimal levels of endogenous MT1-MMP; Supporting Information, Figure S9) were transfected to express wild-type MT1-MMP. Thus, MNC-ActFP exhibited fluorogenic ability in MT1-MMP-expressing MCF-7 cells and a significant signal change was detected over a 60 min incubation. However, mock-transfected MCF-7 cells (vector only) and catalytic mutant MT1-MMP-transfected MCF-7 cells[9] did not exhibit NIR fluoroscence, consistent with the fluorogenic activity depending on the catalytic activity of MT1-MMP. These results indicated that the MNC-ActFP had potential as a dual imaging probe (MR and NIR fluoresence imaging) specifically for MT1-MMP-expressing cancer cells.

To confirm the in vivo diagnostic utility of MNC-ActFP (recognition of protease expression and proteolytic activity), MR and NIR fluorescence imaging of molecular markers was explored using a MT1-MMP-expressing tumor-bearing mouse model. MR imaging for the tumor-bearing mice (1×10^7 HT1080 cells, the proximal thigh region) was performed at different time points (preinjection, 15 min, 1 h, 2 h, and 4 h) after the intravenous injection of MNC-ActFP (200 μg Fe + Mn) into the tail vein. After the injection of MNC-ActFP, an immediate MR signal increase was evident and the signal gradually increased over 4 h. Moreover, MR signal-enhanced microvessels from the tumor were confirmed (red arrow heads in Figure 4a) and 49.7% of the $\Delta R2/R2_{\text{preinjection}}$ value was confirmed at 4 h. In contrast, the control probes (MNC-ScrFP and MNC-ActFP plus inhibitor) showed no enhanced MR signal intensity at the tumor site (Supporting information, Figure S10).

For the multilateral recognition of MT1-MMP-expressing cancer cells, on the other hand, in vivo proteolytic activity based on MNC-ActFP was investigated by NIR fluorescence imaging. Similar to the in vivo MR imaging experiment,

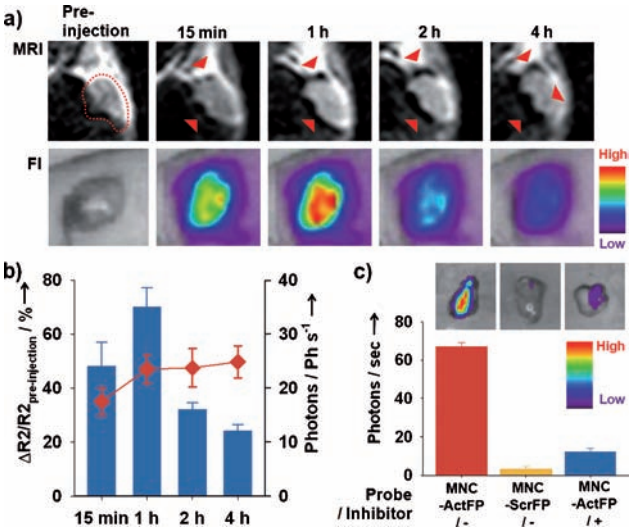

Figure 4. a) In vivo MR (upper) and NIR fluorescence (lower) images of tumor-bearing mice after intravenous injection of MNC-ActFP, MNC-ScrFP, and MNC-ActFP plus inhibitor (200 μg Fe + Mn per mouse) at different time points (preinjection, 15 min, 1 h, 2 h, and 4 h). Red arrowheads in the MR images indicate the signal-enhanced sites of the tumor. b) $\Delta R2/R2_{\text{nontreatment}}$ (line scatter) and NIR fluorescence intensity (bar graphs). c) NIR fluorescence images (upper) and their intensity graph (lower) for excised tumors from tumor-bearing mice 1 h after intravenous injection of MNC-ActFP, MNC-ScrFP, and MNC-ActFP plus inhibitor.

MNC-ActFP was injected intravenously into the tail vein of a MT1-MMP-expressing tumor-bearing mouse model. Sequential NIR fluorescence images ($\lambda_{\text{emission}} = 690$ nm) were obtained for 4 h after the injection of MNC-ActFP and a strong NIR fluorescence signal was seen in tumor sites (Figure 4a, lower panel). The maximum Cy5.5 signal in the tumor site was seen with 35 Ph s^{-1} at 1 h after the injection (Figure 4b). However, the control probes (MNC-ScrFP and MNC-ActFP plus inhibitor) showed no enhanced NIR fluorescence intensity (Supporting Information, Figure S11). Furthermore, depth profiles from the NIR fluorescence images were constructed by examining the intensity in slices cut along the z axis, which represented the two-dimensional slices, starting from $z = 1$ to 7 mm depth. The fluorescence signal in tumor site was maximal between the depths of 3 and 5 mm (Supporting Information, Figure S12). Ex vivo NIR fluorescence imaging for extracted tumor tissue demonstrated that MNC-ActFP showed strong signal intensity in the tumor tissue compared with the other conditions (MNC-ScrFP and MNC-ActFP plus inhibitor; Figure 4c). Notably, the MR signal from MNC-ActFP was maintained for 4 h and the NIR fluorescence signal in tumor tissue was increased at 2 h after the injection of the fluorogenic probe. These results are consistent with the release of Cy5.5 from ActFP after the cleavage by MT1-MMP anchored on invasive cancer cells acting as a NIR fluorescence imaging probe and MNC taken up by cancer cells, by protease-mediated endocytosis, being detected by MR imaging.

In conclusion, we have developed a MT1-MMP-targetable fluorogenic magnetic nanoprobe (MNC-ActFP) for the simultaneous assessment of the expression and proteolytic

activity of MT1-MMP anchored on invasive cancer cells by MR and NIR fluorescence imaging. Trafficking of MT1-MMP as a target biomarker for the molecular imaging provides a matched imaging signal for the detection of invasive cancer cells and early metastatic cancer. Thus, a MT1-MMP-specific peptide sequence (GPLPLRSWGLK) was designed and synthesized to provide fluorogenic activity by the combination of a NIR dye and a quencher to induce a FRET effect. Thus, we believe that the developed nanohybrid, a combined fluorescence imaging probe and MR imaging contrast agent, may be used to increase the sensitivity and specificity of detecting invasive cancer cells in diagnostic and therapeutic interventions in human cancer patients.

Received: September 23, 2011
Published online: December 12, 2011

Keywords: cancer · fluorogenic probes · magnetic resonance imaging · MT1-MMP · nanoprobes

[1] a) T. E. McCann, N. Kosaka, B. Turkbey, M. Mitsunaga, P. L. Choyke, H. Kobayashi, *NMR Biomed.* **2011**, *24*, 561; b) S. Lee, E.-J. Cha, K. Park, S.-Y. Lee, J.-K. Hong, I.-C. Sun, S. Y. Kim, K. Choi, I. C. Kwon, K. Kim, C.-H. Ahn, *Angew. Chem.* **2008**, *120*, 2846; *Angew. Chem. Int. Ed.* **2008**, *47*, 2804.

[2] R. G. Rowe, S. J. Weiss, *Annu. Rev. Cell Dev. Biol.* **2009**, *25*, 567.

[3] K. B. Hotary, E. D. Allen, P. C. Brooks, N. S. Datta, M. W. Long, S. J. Weiss, *Cell* **2003**, *114*, 33.

[4] a) S. Ohkubo, K. Miyadera, Y. Sugimoto, K.-i. Matsuo, K. Wierzba, Y. Yamada, *Biochem. Biophys. Res. Commun.* **1999**, *266*, 308; b) A. R. Clapp, I. L. Medintz, H. Mattoussi, *ChemPhysChem* **2006**, *7*, 47; c) A. Remacle, G. Murphy, C. Roghi, *J. Cell Sci.* **2003**, *116*, 3905.

[5] I. L. Medintz, A. R. Clapp, F. M. Brunel, T. Tiefenbrunn, H. Tetsuo Uyeda, E. L. Chang, J. R. Deschamps, P. E. Dawson, H. Mattoussi, *Nat. Mater.* **2006**, *5*, 581.

[6] a) J.-s. Choi, J. C. Park, H. Nah, S. Woo, J. Oh, K. M. Kim, G. J. Cheon, Y. Chang, J. Yoo, J. Cheon, *Angew. Chem.* **2008**, *120*, 6355; *Angew. Chem. Int. Ed.* **2008**, *47*, 6259; b) L. Frullano, C. Catana, T. Benner, A. D. Sherry, P. Caravan, *Angew. Chem.* **2010**, *122*, 2432; *Angew. Chem. Int. Ed.* **2010**, *49*, 2382; c) S. Mizukami, R. Takikawa, F. Sugihara, M. Shirakawa, K. Kikuchi, *Angew. Chem.* **2009**, *121*, 3695; *Angew. Chem. Int. Ed.* **2009**, *48*, 3641; d) J.-H. Park, G. von Maltzahn, E. Ruoslahti, S. N. Bhatia, M. J. Sailor, *Angew. Chem.* **2008**, *120*, 7394; *Angew. Chem. Int. Ed.* **2008**, *47*, 7284; e) T. D. Schladt, M. I. Shukoor, K. Schneider, M. N. Tahir, F. Natalio, I. Ament, J. Becker, F. D. Jochum, S. Weber, O. Köhler, P. Theato, L. M. Schreiber, C. Sönnichsen, H. C. Schröder, W. E. G. Müller, W. Tremel, *Angew. Chem.* **2010**, *122*, 4068; *Angew. Chem. Int. Ed.* **2010**, *49*, 3976; f) Y. Song, X. Xu, K. W. MacRenaris, X.-Q. Zhang, C. A. Mirkin, T. J. Meade, *Angew. Chem.* **2009**, *121*, 9307; *Angew. Chem. Int. Ed.* **2009**, *48*, 9143; g) M. K. Yu, Y. Y. Jeong, J. Park, S. Park, J. W. Kim, J. J. Min, K. Kim, S. Jon, *Angew. Chem.* **2008**, *120*, 5442; *Angew. Chem. Int. Ed.* **2008**, *47*, 5362; h) M. Nahrendorf, P. Waterman, G. Thurber, K. Groves, M. Rajopadhye, P. Panizzi, B. Marinelli, E. Aikawa, M. J. Pittet, F. K. Swirski, R. Weissleder, *Arterioscler. Thromb. Vasc. Biol.* **2009**, *29*, 1444.

[7] S. Lee, K. Park, S.-Y. Lee, J. H. Ryu, J. W. Park, H. J. Ahn, I. C. Kwon, I.-C. Youn, K. Kim, K. Choi, *Bioconjugate Chem.* **2008**, *19*, 1743.

[8] a) J. Yang, C.-H. Lee, H.-J. Ko, J.-S. Suh, H.-G. Yoon, K. Lee, Y.-M. Huh, S. Haam, *Angew. Chem.* **2007**, *119*, 8992; *Angew. Chem. Int. Ed.* **2007**, *46*, 8836; b) E.-K. Lim, J. Yang, J.-S. Suh, Y.-M. Huh, S. Haam, *J. Mater. Chem.* **2009**, *19*, 8958.

[9] R. C. Domingues, M. P. Carneiro, F. C. R. Lopes, R. C. Domingues, L. M. B. da Fonseca, E. L. Gasparetto, *Am. J. Roentgenol.* **2009**, *192*, 1012.

